Research Article | Vol. 25, No. 16 | 7 Aug 2017 | OPTICS EXPRESS 19251
Optics EXPRESS

Broadband Fourier-transform spectrometer enabling modal subset identification in Fabry-Pérot-based astrocombs

JAKE M. CHARSLEY,* RICHARD A. MCCRACKEN, LAUREN REID, AND DERRYCK T. REID

Scottish Universities Physics Alliance (SUPA), Institute of Photonics and Quantum Sciences, School of Engineering and Physical Sciences, Heriot-Watt University, Edinburgh EH14 4AS, UK
**jc50@hw.ac.uk*

Abstract: A multi-GHz frequency comb (astrocomb) is typically realized by filtering modes of a sub-GHz frequency comb (source comb) in a Fabry-Pérot etalon, which can lead to ambiguities in determining which subset of source comb modes has been filtered. Here we demonstrate a broadband Fourier-transform spectrometer (FTS) with a resolving power of R = 430,000 at 550 nm, and apply it to the identification of comb subsets from a filtered 1-GHz supercontinuum. After apodization the FTS demonstrated an instrument line shape width of 1.26 GHz which enabled individual comb-line positions to be identified with an uncertainty of 17.6 MHz, a relative precision of 5×10^{-8}. Correcting for air dispersion allowed the instrument to determine the comb-mode spacing to an accuracy of 300 Hz and filtered subsets of source comb modes to be uniquely distingished across the entire comb bandwidth from 550 to 900 nm. The inherently broadband design of the FTS makes it suitable in future applications for calibrating ultra-broadband astrocombs employed by instruments such as ELT HIRES.

OCIS codes: (120.4640) Optical instruments; (300.6300) Spectroscopy, Fourier transforms; (350.1260) Astronomical optics.

References and links

1. T. Steinmetz, T. Wilken, C. Araujo-Hauck, R. Holzwarth, T. W. Hänsch, L. Pasquini, A. Manescau, S. D'Odorico, M. T. Murphy, T. Kentischer, W. Schmidt, and T. Udem, "Laser frequency combs for astronomical observations," Science **321**(5894), 1335–1337 (2008).
2. C.-H. Li, A. J. Benedick, P. Fendel, A. G. Glenday, F. X. Kärtner, D. F. Phillips, D. Sasselov, A. Szentgyorgyi, and R. L. Walsworth, "A laser frequency comb that enables radial velocity measurements with a precision of 1 cm s(-1)," Nature **452**(7187), 610–612 (2008).
3. A. G. Glenday, C.-H. Li, N. Langellier, G. Chang, L.-J. Chen, G. Furesz, A. A. Zibrov, F. Kärtner, D. F. Phillips, D. Sasselov, A. Szentgyorgyi, and R. L. Walsworth, "Operation of a broadband visible-wavelength astro-comb with a high-resolution astrophysical spectrograph," Optica **2**(3), 250–254 (2015).
4. R. A. McCracken, É. Depagne, R. B. Kuhn, N. Erasmus, L. A. Crause, and D. T. Reid, "Wavelength calibration of a high resolution spectrograph with a partially stabilized 15-GHz astrocomb from 550 to 890 nm," Opt. Express **25**(6), 6450–6460 (2017).
5. A. Bartels, D. Heinecke, and S. A. Diddams, "10-GHz self-referenced optical frequency comb," Science **326**(5953), 681 (2009).
6. M. Endo, I. Ito, and Y. Kobayashi, "Direct 15-GHz mode-spacing optical frequency comb with a Kerr-lens mode-locked Yb:Y(2)O(3) ceramic laser," Opt. Express **23**(2), 1276–1282 (2015).
7. J. M. Charsley, R. A. McCracken, D. T. Reid, G. Kowzan, P. Masłowski, A. Reiners, and P. Huke, "Comparison of astrophysical laser frequency combs with respect to the requirements of HIRES," in *Proc. SPIE, Optical Measurement Systems for Industrial Inspection X* (2017), pp. 10329–10333.
8. R. A. McCracken, J. M. Charsley, and D. T. Reid, "A decade of astrocombs: recent advances in frequency combs for astronomy," Opt. Express **25**(13), 15058–15078 (2017).
9. C.-H. Li, G. Chang, A. G. Glenday, N. Langellier, A. Zibrov, D. F. Phillips, F. X. Kärtner, A. Szentgyorgyi, and R. L. Walsworth, "Conjugate Fabry-Perot cavity pair for improved astro-comb accuracy," Opt. Lett. **37**(15), 3090–3092 (2012).
10. C.-H. Li, A. G. Glenday, A. J. Benedick, G. Chang, L.-J. Chen, C. Cramer, P. Fendel, G. Furesz, F. X. Kärtner, S. Korzennik, D. F. Phillips, D. Sasselov, A. Szentgyorgyi, and R. L. Walsworth, "In-situ determination of astro-

#293417 https://doi.org/10.1364/OE.25.019251
Journal © 2017 Received 2 May 2017; revised 26 Jun 2017; accepted 26 Jun 2017; published 1 Aug 2017

Optics EXPRESS

comb calibrator lines to better than 10 cm s-1," Opt. Express **18**(12), 13239–13249 (2010).
11. G. G. Ycas, F. Quinlan, S. A. Diddams, S. Osterman, S. Mahadevan, S. Redman, R. Terrien, L. Ramsey, C. F. Bender, B. Botzer, and S. Sigurdsson, "Demonstration of on-sky calibration of astronomical spectra using a 25 GHz near-IR laser frequency comb," Opt. Express **20**(6), 6631–6643 (2012).
12. T. Steinmetz, T. Wilken, C. Araujo-Hauck, R. Holzwarth, T. W. Hänsch, and T. Udem, "Fabry–Pérot filter cavities for wide-spaced frequency combs with large spectral bandwidth," Appl. Phys. B **96**(2-3), 251–256 (2009).
13. A. Marconi, P. Di Marcantonio, V. D'Odorico, S. Cristiani, R. Maiolino, E. Oliva, L. Origlia, M. Riva, L. Valenziano, F. M. Zerbi, M. Abreu, V. Adibekyan, C. Allenda Prieto, P. J. Amado, W. Benz, I. Boisse, X. Bonfils, F. Bouchy, D. Buscher, A. Cabral, B. L. Canto Martins, A. Chiavassa, J. Coelho, E. Delgado, J. R. De Medeiros, I. Di Varano, P. Figueira, M. Fisher, J. P. U. Fynbo, A. C. H. Glasse, M. Haehnelt, C. Haniff, A. Hatzes, P. Huke, A. J. Korn, I. C. Leao, J. Liske, C. Lovis, I. Matute, R. A. McCracken, C. J. A. P. Martins, M. J. P. F. G. Monteiro, S. Morris, T. Morris, H. Nicklas, A. Niedzielski, N. Nunes, E. Palle, P. Parr-Burman, V. Parro, I. Parry, F. Pepe, N. Piskunov, D. Queloz, A. Quirrenbach, R. Rebolo Lopez, A. Reiners, D. T. Reid, N. Santos, W. Seifert, S. Sousa, H. C. Stempels, K. Strassmeier, X. Sun, S. Udry, M. Weber, and E. Zackrisson, "EELT-HIRES the high-resolution spectrograph for the E-ELT," Proc. SPIE **9908**, 990823 (2016).
14. A. Zybin, J. Koch, H. D. Wizemann, J. Franzke, and K. Niemax, "Diode laser atomic absorption spectrometry," Spectrochim. Acta B At. Spectrosc. **60**(1), 1–11 (2005).
15. G. Galbács, "A review of applications and experimental improvements related to diode laser atomic spectroscopy," Appl. Spectrosc. Rev. **41**(3), 259–303 (2006).
16. A. G. Glenday, D. F. Phillips, M. Webber, C.-H. Li, G. Furesz, G. Chang, L.-J. Chen, F. X. Kärtner, D. D. Sasselov, A. H. Szentgyorgyi, and R. L. Walsworth, "High-resolution Fourier transform spectrograph for characterization of echelle spectrograph wavelength calibrators," Proc. SPIE **8446**, 844696 (2012).
17. A. G. Glenday, C.-H. Li, N. Langellier, G. Chang, L.-J. Chen, G. Furesz, A. A. Zibrov, F. Kärtner, D. F. Phillips, D. Sasselov, A. Szentgyorgyi, and R. L. Walsworth, "Operation of a broadband visible-wavelength astro-comb with a high-resolution astrophysical spectrograph: supplementary material," Optica **2**(3), S1–S6 (2015).
18. V. Tsatourian, H. S. Margolis, G. Marra, D. T. Reid, and P. Gill, "Common-path self-referencing interferometer for carrier-envelope offset frequency stabilization with enhanced noise immunity," Opt. Lett. **35**(8), 1209–1211 (2010).
19. Z. Zhang, K. Balskus, R. A. McCracken, and D. T. Reid, "Mode-resolved 10-GHz frequency comb from a femtosecond optical parametric oscillator," Opt. Lett. **40**(12), 2692–2695 (2015).
20. J. Ye, S. Swartz, P. Jungner, and J. L. Hall, "Hyperfine structure and absolute frequency of the (87)Rb 5P(3/2) state," Opt. Lett. **21**(16), 1280–1282 (1996).
21. P. E. Ciddor, "Refractive index of air: new equations for the visible and near infrared," Appl. Opt. **35**(9), 1566–1573 (1996).
22. M. S. Bartlett, "Periodogram analysis and continuous spectra," Biometrika **37**(1-2), 1–16 (1950).
23. L. Rutkowski, P. Masłowski, A. C. Johansson, A. Khodabakhsh, and A. Foltynowicz, "Optical frequency comb Fourier transform spectroscopy with sub-nominal resolution," arXiv:1612.04808 (2016).
24. C. H. Knapp and G. C. Carter, "The generalized correlation method for estimation of time delay," IEEE Trans. Acoust. **24**(4), 320–327 (1976).
25. B. C. Smith, *Fundamentals of Fourier Transfom Spectroscopy* (CRC, 1996).
26. Spectratime, "iSource +^{TM} Ultra LCR-900 Spec," www.spectratime.com/documents/lcr_spec.pdf.
27. "D2-100 DBR laser spec," http://www.vescent.com/products/lasers/d2-100-dbr-laser.
28. "PDA36A spec," https://www.thorlabs.com/thorproduct.cfm?partnumber=PDA36A-EC.
29. N. B. Hébert, S. K. Scholten, R. T. White, J. Genest, A. N. Luiten, and J. D. Anstie, "A quantitative mode-resolved frequency comb spectrometer," Opt. Express **23**(11), 13991–14001 (2015).

1. Introduction

The past decade has seen the development of various astrocomb architectures for astronomical spectrograph calibration [1–4] which exploit the stability and narrow linewidth of a frequency comb and deploy it as an optical ruler. The precisely-known frequency spacings of the comb lines are used to produce a wavelength solution of the cross-dispersed light that is incident on the CCD array of a high-resolution echelle spectrograph, enabling the identification of systematic errors and long-term instrument drifts.

The optimal mode spacing for an astrocomb is determined by the resolving power of the spectrograph $R = \lambda/\Delta\lambda$ (normally > 40,000) and is typically 5–40 GHz, a repetition frequency range that is itself only achievable directly from a mode-locked laser in a few select cases [5,6], and at which the reduced peak powers become problematic for spectral broadening and other nonlinear conversion techniques. The prevailing approach to achieve a multi-GHz mode spacing is to filter the modes of a lower-repetition-rate laser in a Fabry-Pérot etalon (FP), and this technique has been used in every deployed astrocomb to date [7,8]. The filtering of a

Optics EXPRESS

frequency comb is non-trivial, and consideration of the etalon mirror coatings and curvature is necessary to ensure that unwanted modes are sufficiently suppressed [9,10].

An ambiguity exists in determining which subset of modes has been filtered from the dense source comb, as shown in Fig. 1(a). A common approach to address this problem for narrowband filtered combs has been to use a laser diode as an optical reference, locking it directly to (or beating it against) a comb tooth [11,12]. A wavemeter and an RF spectrum analyzer can provide sufficient diagnostic information to identify this comb tooth, from which the frequencies of the other comb modes can be calculated. The diode laser is then used to stabilize the Fabry-Pérot etalon, and therefore transmission of this reference laser also ensures transmission of a known subset of comb modes. This approach is only suitable for astrocomb systems comprising one Fabry-Pérot etalon (or set of etalons which filter a comb multiple times). Next-generation high resolution spectrographs demand extremely-broadband spectral coverage, such as the forthcoming HIRES instrument for the ELT [13] therefore multiple Fabry-Pérot etalons will need to be employed to provide the required modal spacing in each wavelength band [7]. Each etalon could therefore filter a different subset of comb modes which would lead to discontinuities at the edge of each wavelength band where the two subsets would overlap. Additionally, the approach of referencing all cavities to laser diodes is denied due to an absence of available narrow-linewidth sources and atomic references systematically spaced across the UV to the IR coverage [14,15].

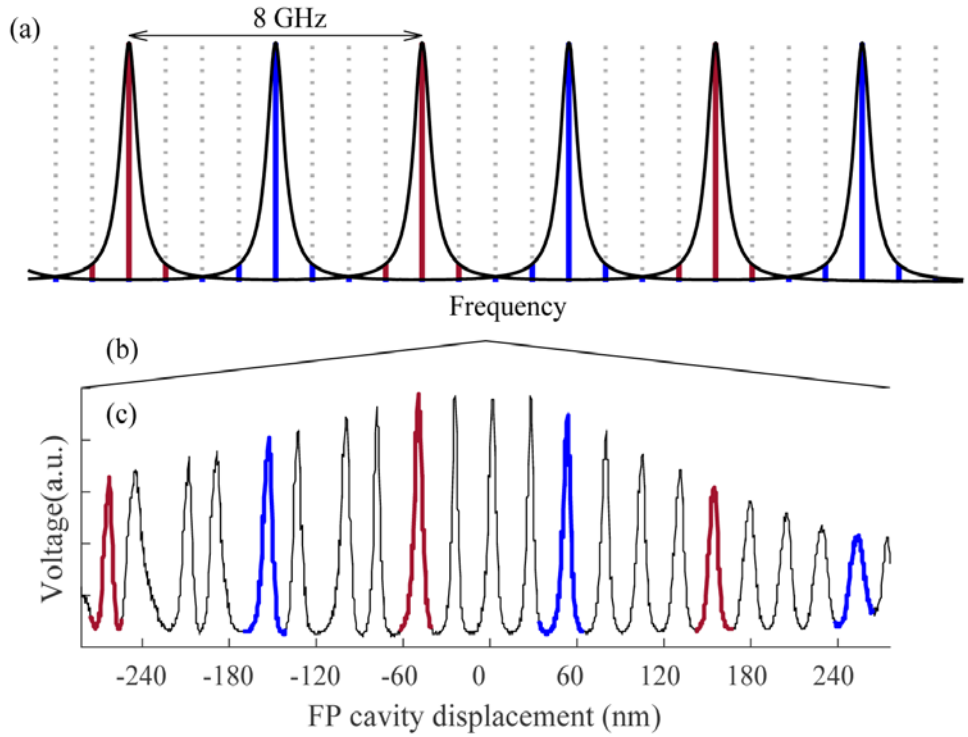

Fig. 1. (a) A Fabry-Pérot etalon can filter any subset of modes from a dense source comb. Here we illustrate two possible 8-GHz subsets selected from a 1-GHz comb. (c) The transmission profile of the Fabry-Pérot etalon as its length is swept by the triangular wave shown in (b). Red and blue lines indicate different 8-GHz subsets of the 1-GHz comb.

Here we demonstrate modal subset identification of an extremely-broadband astrocomb with a compact Fourier transform spectrometer (FTS). Previous examples of astrocombs deployed on an FTS have focused on employing high resolution (<100 MHz) instruments to characterize sideband suppression [16,17], requiring large optical paths and extreme

Optics EXPRESS

environmental stability. The compact FTS we report here is capable of resolving the modes of a supercontinuum pumped by a 1-GHz Ti:sapphire frequency comb, which are filtered by a Fabry-Pérot etalon locked to a comb transmission peak. The FTS path length is calibrated with an atomically-referenced diode laser and provides repeatable results from lock-to-lock, making it a promising on-site diagnostic tool for modal subset identification in broadband astrocombs for calibration of next-generation astronomical spectrographs for high-precision radial velocity measurements.

2. Experiment

The experimental layout is depicted in Fig. 2. Below we describe stabilization of the frequency comb and Fabry-Pérot etalon, and the design and operation of the FTS.

2.1 Frequency comb stabilization

A 1-GHz Ti:sapphire laser (Gigajet, Laser Quantum) produced 30-fs pulses with a central wavelength of 808 nm and 1.2-W average power. Approximately 500 mW was focused into a 12-cm-long photonic crystal fiber (PCF, FemtoWhite 800, NKT Photonics) with 70% coupling efficiency to generate an octave-spanning supercontinuum. Pre-compensation with dispersive mirrors ensured transform-limited pulses at the input facet of the PCF, maintaining supercontinuum phase coherence.

A dichroic mirror directed wavelengths from 550 to 900 nm towards the Fabry-Pérot etalon (see §2.2), with spectral components outside this range steered into a common-path f-to-2f interferometer with a design similar to that reported in [18] and illustrated in Fig. 2(c). A polarizer ensured a horizontal polarization at both visible and infrared wavelengths. Both spectral components were focused into a 2-mm-long LBO crystal cut for Type I SHG of 1060 nm, producing two orthogonally-polarized pulse sequences at 530 nm that propagated co-linearly. These pulses were focused into a Wollaston prism, splitting the polarizations with a 5° separation angle. The prism provided a differential group delay between the orthogonal polarizations, compensating for the group delay introduced within the PCF between the 1060-nm and 530-nm spectral components. The expanding beams were imaged back into the prism using a spherical silver mirror, and a slight vertical displacement allowed the recombined beams to be collected and directed towards an avalanche photodiode (APD430A2, Thorlabs). An interference filter with a 10-nm bandwidth removed unwanted spectral components, and a polarizer was used to balance the optical power between the fundamental and frequency-doubled 530-nm beams. The detected carrier-envelope offset frequency (f_{CEO}) had a 30-dB signal-to-noise ratio (SNR), sufficient for long-term monitoring. A stronger SNR is readily achievable with this interferometer, however the dichroic mirror used to direct light to the Fabry-Pérot etalon did not provide uniform reflectivity at the 530-nm and 1030-nm wavelengths required for beat detection. Previous measurements of f_{CEO} in this laser demonstrated a passive stability of 2.4 MHz hr^{-1} [4], thus active stabilization was not required for the purposes of the FTS demonstration. Detection of the repetition frequency (f_{REP}) was achieved by focusing a portion of the remaining Ti:sapphire power into a high-bandwidth GaAs photodiode (ET-3500, Electro-Optics Technology). The 8th harmonic of f_{REP} was compared against an RF synthesizer (FSL-0010, QuickSyn Lite), and the error signal used to provide feedback to a pair of piezoelectric transducers actuating mirror positions in the Ti:sapphire laser cavity.

Optics EXPRESS

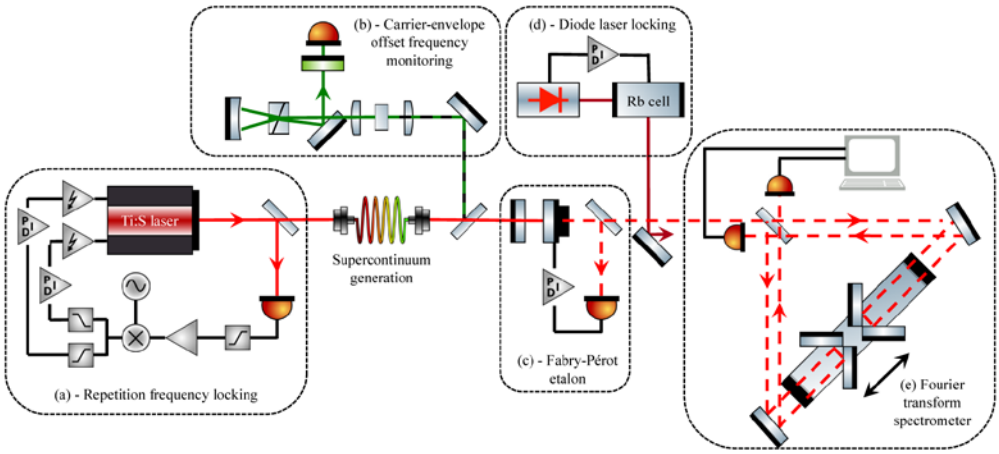

Fig. 2. Optical configuration of the experiment. (a), Ti:sapphire laser with f_{REP} locking loop. (b), common path *f*-to-2*f* interferometer for f_{CEO} detection. (c), Fabry-Pérot etalon stabilized to a transmission peak. (d), narrow linewidth diode laser locked to a rubidium absorption line. (e), folded Fourier-transform spectrometer.

The design of the Fabry-Pérot etalon was identical to that reported in [4]. A pair of 98% reflectivity mirrors with complementary-dispersive coatings provided flat group delay across the 550–900nm region (Laseroptik). The cavity finesse of $F = 155$ provided a balance between sideband suppression and broadband operation. The etalon spacing was tuned to support an 8-GHz free spectral range, filtering the 1-GHz comb from the laser by a factor of eight. A triangular scan signal was applied to a 100-µm-travel piezoelectric actuator (NPM140, Newport) on which was mounted one of the etalon mirrors. Scanning the etalon spacing in this manner revealed the transmission profile shown in Fig. 1(c), with each transmission peak corresponding to an 8-GHz subset of the 1-GHz source-comb mode spacing. Dither locking was employed to stabilize the etalon spacing to a chosen transmission peak of the comb, providing a tight lock with sub-MHz uncertainty in the transmitted mode spacing.

2.2 Fourier transform spectrometer

The Fourier transform spectrometer is shown in Fig. 2(e). The design was based on that reported in [19] and comprised a pair of corner-cube retroreflectors mounted back-to-back on a long-travel motorized stage (DDSM100, Thorlabs), allowing the optical path difference (OPD) in each arm to be changed simultaneously and in opposite directions, effectively providing a 4-fold increase in the travel range of the stage for a spectral resolution as high as 750 MHz. Broadband operation was achieved by using all-metallic folding mirrors and a partially-silvered beam splitter, providing a linear instrument response with respect to chromatic dispersion. With appropriate dichroic beam splitters and detectors in the exit channel(s) of the FTS, this all-metallic design would enable astrocomb analysis from the UV to the mid-IR, however here we limit our measurements to the operational range of our Fabry-Pérot filter cavity.

Detection of the filtered comb was implemented using a pair of amplified silicon photodiodes (PDA36A-EC, Thorlabs), and the data acquired using a 16-bit USB oscilloscope at a sampling rate of 6.25 MS/s (Handyscope HS5, TiePie engineering). The OPD was calibrated using a narrow-linewidth single frequency diode laser (D2-100-DBR, Vescent Photonics) dither-locked to the ^{87}Rb $F = 2 \rightarrow F' = 2,3$ crossover [20], providing absolute frequency traceability. Comb light detection and OPD calibration were carried out simultaneously to correct for stage jitter, with the filtered comb light and reference laser coupled into the FTS in a collinear, near-co-propagating geometry.

Optics EXPRESS

3. Data retrieval

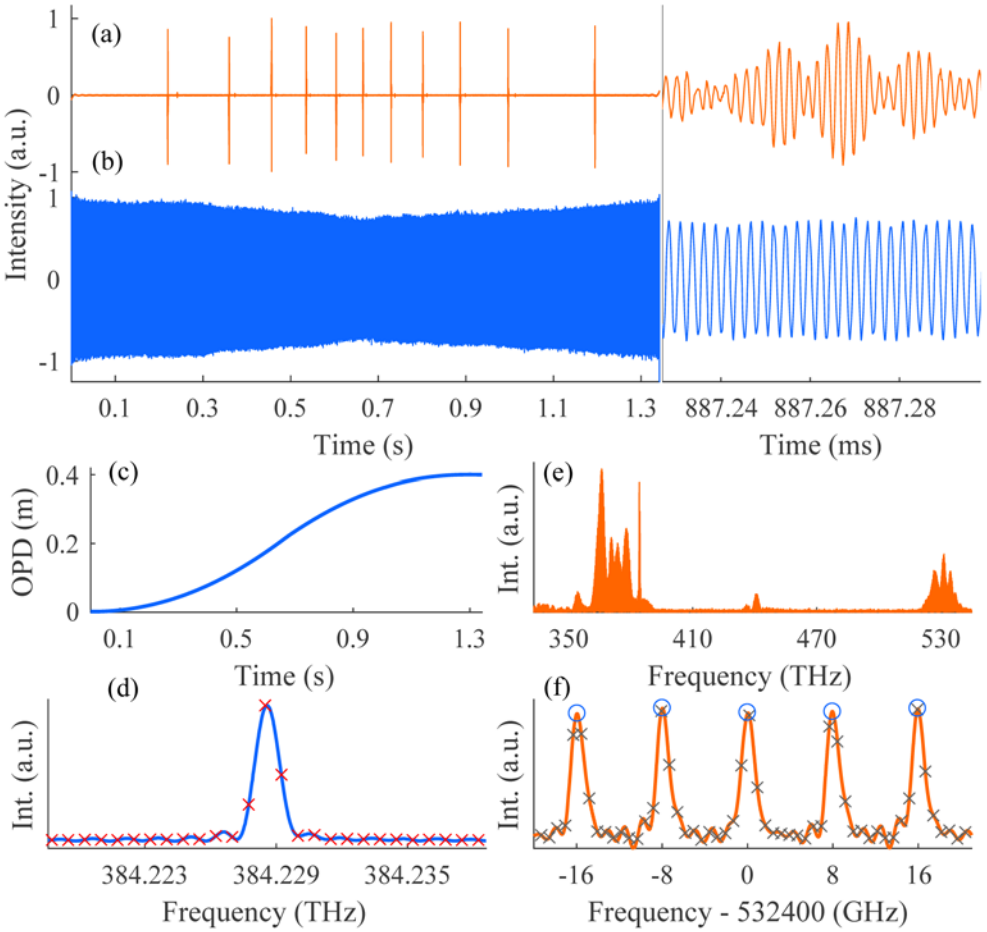

Fig. 3. FTS analysis protocol. Panels (a) and (b) show the balanced comb interferogram signal and the reference interferogram signal (centered about zero) respectively, over the course of the scan. The input is a 1-GHz supercontinuum FP-filtered to 8 GHz. Panel (c) illustrates the stage displacement over the scan calibrated by applying a zero-crossing algorithm to the reference signal. The instrument line shape of the spectrometer is revealed by upsampling the unresolved Rb spectral line (1.27-GHz apodized line width) shown in Panel (d). Panel (e) shows the retrieved supercontinuum spectrum. Finally, Panel (f) shows a selection of filtered comb modes, upsampled to illustrate the similarity of their line shapes with the instrument response. Cross-correlation was employed to find the peak positions (circled in blue).

The analysis protocol for the Fourier transform spectrometer is outlined in Fig. 3, which shows data for a Ti:sapphire supercontinuum comb, and the retrieval methodology is described below. Three signals were recorded for each scan of the FTS: the reference signal from the Rb-stabilized diode laser, and two anti-phase interferogram signals from the filtered frequency comb for balanced detection.

Firstly, the scan profile of the OPD was characterized using the reference signal, which was low-pass filtered to center the single-frequency oscillations about zero. An algorithm was applied to identify the half-fringe spacing across the scan, with upsampling by a factor of four utilized to increase the accuracy of the 'zero-crossing' positions in the central region of the scan (where the sampling is the most strained). These zero-crossing positions correspond to a half-wavelength separation of the interfering Rb-reference beams propagating in air, with the reference wavelength given by $\lambda_{REF} = \lambda_{Rb}/n_{air}$ (λ_{Rb}) where λ_{Rb} = 780.2465(8) nm is the Rb-

Optics EXPRESS

referenced wavelength of the narrow-line diode laser [20] and n_{air} is the refractive index of air given in the relations provided by Ciddor [21]. Using this method we characterized the optical path difference for the scan, with the maximum OPD of 40 cm corresponding to an unapodized instrument-limited resolution of 750 MHz.

As the linewidth of the diode laser is much narrower than the instrument-limited resolution, the line shape of the reference is unresolved by the FTS. The characteristic line shape of the instrument can therefore be determined from a Fourier transform of the reference interferogram. Characterization of the instrument line shape permits a thorough analysis of the modes of the FP-filtered frequency comb and is discussed in §4. In obtaining the instrument line shape the reference interferogram was linearly resampled in delay, apodized, and a fast Fourier transform (FFT) applied. The instrument line shape is affected by the chosen apodization function. We chose to implement a triangular apodization function on the reference signal which corresponds to an instrument line shape with a sinc^2 dependence [22].

The interferogram signals from the FP-filtered frequency comb were subjected to a similar low-pass filtering process and then balanced detection was implemented by subtracting one interferogram signal from the other. The resulting single comb interferogram was upsampled by the same factor used in the reference analysis and linearly resampled in delay with use of the obtained OPD profile. The comb interferogram was apodized and a FFT performed to retrieve the filtered comb modes. The same triangular apodization function used to condition the reference signal was imposed on the comb interferogram to ensure a consistent instrument line shape between the two retrieved spectra.

The frequency axis is determined by the maximum change in optical path. Compensation of the effects of dispersion of air throughout the spectrum was achieved through use of the relation [23]:

$$\lambda(air) = \lambda(vac)\frac{n_{air}(\lambda)}{n_{air}(\lambda = \lambda_{Rb})} \tag{1}$$

The frequency grid was converted to wavelength where the air dispersion compensation was performed, and then converted back to frequency. This step is vital for analysis of a broadband frequency comb where the wavelength dependence of the dispersion of air has the effect of displacing the retrieved mode positions from their true positions in a nonlinear way across the spectrum.

4. Results and discussion

4.1 Filtered subset identification

Analysis was performed of a Fabry-Pérot-filtered Ti:sapphire supercontinuum ranging in wavelength from 550 to 900 nm and with a mode spacing of 8 GHz. The 1.27-GHz apodized resolution is sufficient to distinguish neighboring subsets, and in Fig. 4 we present results demonstrating the identification of the possible modal subsets from the filtered comb structure near 560 nm. In the experiment, the Fabry-Pérot etalon was locked to all but one of the eight highest transmission peaks, shown in Fig. 1(b), with distinct subsets of the fundamental comb modes identified using the FTS for each lock. As Fig. 4 illustrates, the comb lines obtained for each different Fabry-Pérot lock lie on unique 8-GHz grids, with each grid displaced by a multiple of 1 GHz from the others, exactly as would be expected.

Optics EXPRESS

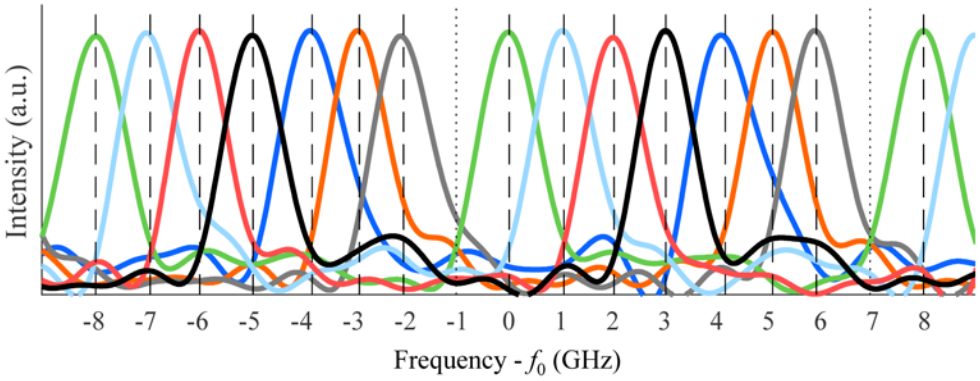

Fig. 4. Modal subset identification. A selection of the retrieved filtered comb modes near 560 nm are displayed. Each of the colored lines represents a distinct subset of the source-comb modes, where seven of the eight possible subsets were generated and identified in the experiment. The 8-GHz mode spacing is consistent with the FSR from the etalon mirror separation. The comb modes are displayed on a frequency scale centered at $f_0 = c$ / 560 nm.

The inherent broadband operation of the FTS is illustrated in Fig. 5. Interferograms were acquired for two neighboring transmission peaks of the Fabry-Pérot etalon. The corresponding upsampled comb spectra, displayed in red and blue in Fig. 5, show a 1-GHz difference in their comb-mode positions across the entire operating bandwidth of the Fabry-Pérot etalon (550–900nm). It is important to note that without correcting for the dispersion of air, the relative spacing between retrieved subsets would exhibit errors across this bandwidth.

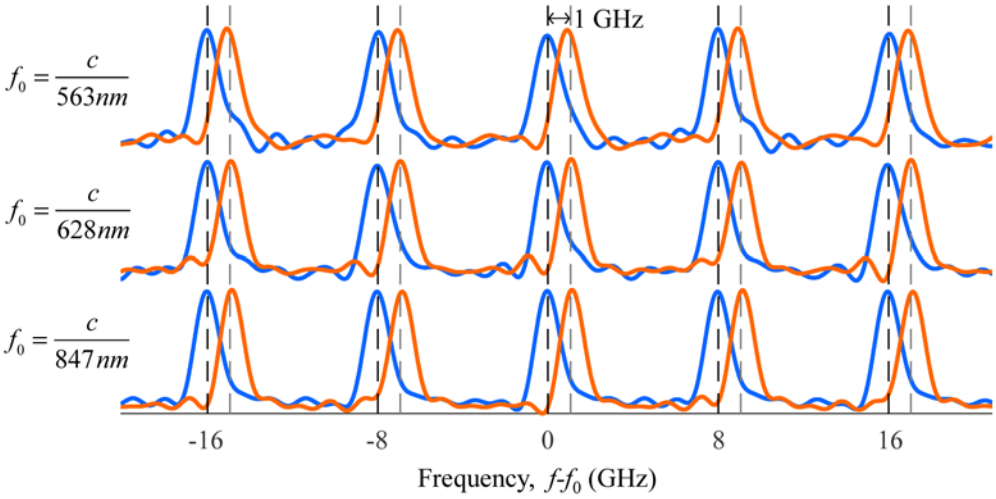

Fig. 5. A 1-GHz separation in the comb-mode positions of neighboring filtered subsets was identified across the full operational bandwidth of the Fabry-Pérot etalon. To allow inter-comparisons, each set of comb modes is displayed on a frequency scale centered at a different frequency, f_0.

4.2 Optical precision

In §4.1 we demonstrated that the instrument response of the FTS is sufficient for modal subset identification, however it is instructive to determine the precision to which the FTS can identify a single filtered comb line. Here we perform an analysis of the optical precision of the FTS, noting that this characterization need not be carried out for each use of the instrument.

The line shape of the instrument characterized by the unresolved Rb reference line enables a quantitative analysis of the retrieved comb-mode positions. The center frequency of each

Optics EXPRESS

comb mode in the supercontinuum (about 6000 in total) was obtained by a cross-correlation analysis with the instrument line shape, following the approach outlined in [24]. This is made possible because the comb modes and the Rb-referenced diode laser share a similar sub-MHz linewidth, neither of which is resolvable by the spectrometer. The cross-correlation technique effectively sweeps the instrument line shape through the comb spectrum, accurately registering the center positions of the comb modes, which correspond to local maxima of the cross-correlation function. The method guarantees a consistent way of obtaining the comb mode frequencies and also, as the instrument line shape is individually characterized for each scan, is insensitive to small differences in the instrument line shape observed from scan to scan. To obtain a clearer representation of the instrument line shape, the Rb-referenced diode laser line and the comb spectrum were upsampled by a factor of 128; the results shown in Fig. 3(d) and 3(f) illustrate the expected sinc^2 character of the instrument line function.

To evaluate the repeatability of the comb-line identification process we blocked the supercontinuum and steered a portion of the unbroadened Ti:sapphire comb into the Fabry-Pérot etalon, which was stabilized to a single transmission peak. We acquired 150 data sets over a 1-hour period, during which time both the Fabry-Pérot etalon and f_{REP} remained locked. A single filtered comb line near 371 THz was isolated and the peak of the comb line determined using the cross-correlation method described in §4.1. The distribution of the retrieved single mode position from each data set is shown in Fig. 6(a). The comb line was identified with a standard deviation of 17.6 MHz (bright red region), corresponding to a 5×10^{-8} relative precision. The extension of this approach to provide the standard deviation in the positions of 1000 comb modes over 150 acquisitions is shown in Fig. 6(b). The slight decrease in precision at lower frequencies may be attributable to imperfect compensation for air dispersion in the FTS, as higher frequencies lie closer to the reference wavelength of ~780.2 nm. With improved monitoring of local environmental conditions the compensation of air dispersion in the FTS can be more accurately applied, preventing a degradation of precision far from the reference wavelength.

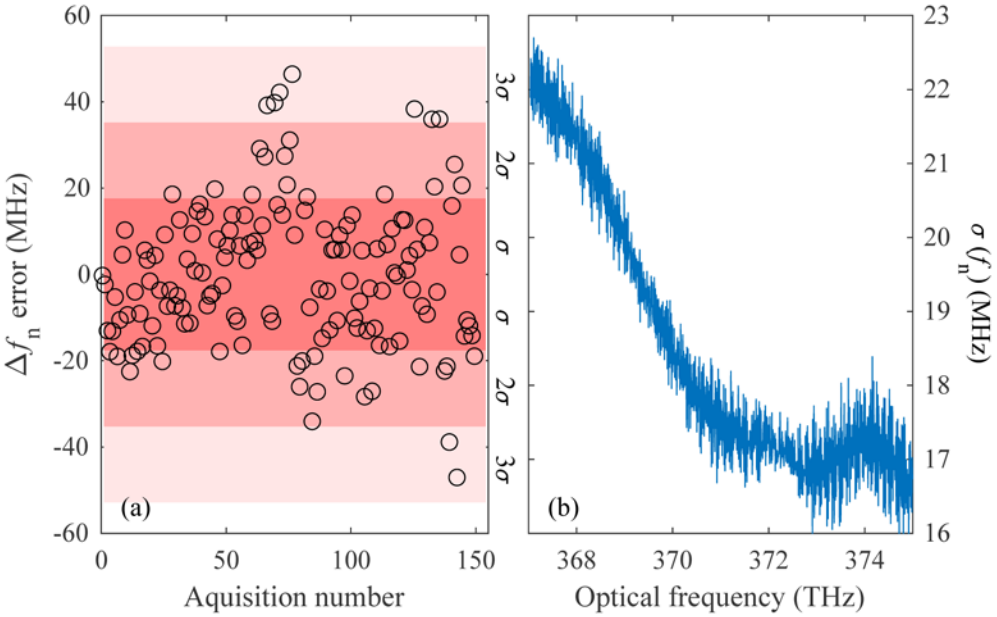

Fig. 6. (a) Uncertainty in the peak position of a single comb line near 371 THz, extracted from 150 data sets. Colored segments indicate standard deviations from the mean. (b) Standard deviations in the positions of each comb line from 367 to 375 THz, extracted from 150 data sets.

Optics EXPRESS

Additional data from multiple filtered subsets were acquired using the Ti:sapphire laser in order to determine the accuracy to which the FTS could identify the mode spacing of the astrocomb under test. This property is critical when analyzing combs in the UV-visible region, as they require extremely wide mode spacings (>40 GHz) and therefore very compact Fabry-Pérot etalons, where the change in mirror separation separating consecutive filter ratios is <100 μm. The peaks of 1000 comb modes were identified for 450 data sets recorded over three hours and the data combined to form a single data set containing the mean positions of 1000 comb modes. The frequency difference Δ between adjacent comb modes is a direct optical measurement of $8f_{REP}$, and this value was obtained for each data set by averaging the spacings between the 1000 comb modes. Conveniently, the laser repetition frequency was stabilized to the 8th harmonic of f_{REP} using a RF synthesizer (frequency, f_{SYNTH}), allowing us simply to subtract f_{SYNTH} from Δ in order to determine the accuracy to which $8f_{REP}$ could be measured using the FTS. Figure 7 shows the deviation between the synthesizer frequency and the optically calculated value of $8f_{REP}$. The mean mode spacing was found to be accurate to within 2.4 kHz of f_{SYNTH} (equivalent to optically determining f_{REP} to within 300 Hz) and the standard deviation was 26 kHz, indicating a 3×10^{-7} precision. It should be noted that the applied compensation for air dispersion is dependent on multiple variables, including air pressure, temperature, water vapor pressure and CO_2 concentration [16]. As such, the accuracy and precision stated here may decrease in any environment unless attention is paid to careful monitoring of local conditions.

The kHz-level and MHz-level uncertainties in the optically retrieved values for f_{REP} and f_n, respectively, are more than sufficient to consistently distinguish the filtered subset of an astrocomb, however limiting systematic uncertainties prevent direct optical retrieval of the carrier envelope offset (CEO) frequency, f_{CEO}. An additional measurement is therefore required to determine whether the CEO frequency measured with the *f*-to-2*f* interferometer is f_{CEO} or f_{REP}-f_{CEO}, such as heterodyning the Ti:sapphire laser with the Rb-referenced diode laser.

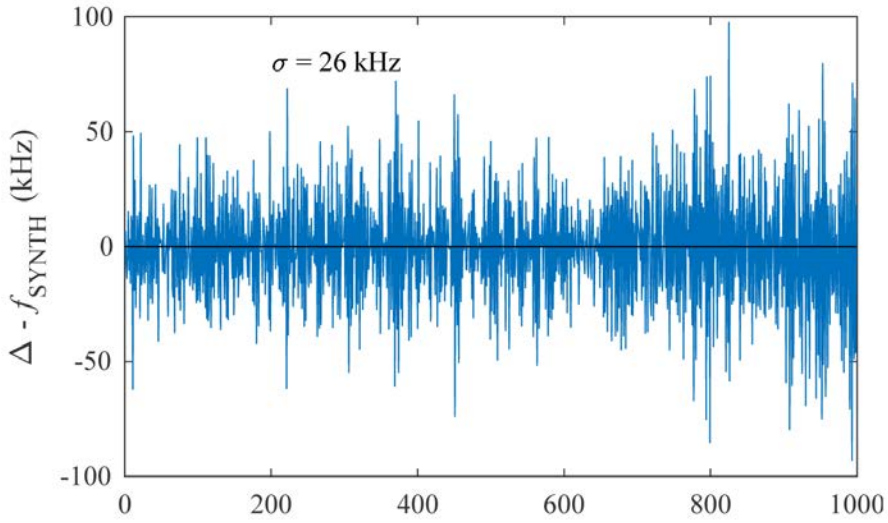

Fig. 7. Difference between the RF synthesizer frequency used for repetition rate stabilization (f_{SYNTH}) and the mean mode spacing between 1000 filtered comb modes ($8f_{REP}$) for 450 data sets. The standard deviation is 26 kHz and the mean offset of $8f_{REP}$ from f_{SYNTH} is 2.4 kHz, equivalent to optically determining f_{REP} with an accuracy of 300 Hz.

Sources of uncertainty in the instrument are listed in Table 1 along with an estimation of their contributions in the optical domain. The RF synthesizer was referenced to a Rb quartz oscillator with 5×10^{-11} accuracy and 3×10^{-11} precision over 1 second, which together with the locking loop used to stabilize f_{REP} results in a 300 Hz uncertainty at 384 THz (~780.2 nm). The diode laser had an approximate linewidth of 1 MHz, and was stabilized to an optical

Optics EXPRESS

transition with estimated line-position uncertainty of <1/200 of the 6-MHz linewidth. The reference laser module contributes an uncertainty of 1.06 MHz at optical frequencies. The carrier envelope offset frequency of the Ti:sapphire laser was not stabilized, resulting in a 1-MHz uncertainty over the 1-second acquisition time. Minute variations in air dispersion as a result of temperature and humidity fluctuations in the FTS resulted in changes to the OPD at each frequency, displacing the comb modes upon retrieval. While instantaneous changes will be very small, n_{air} changes by 10^{-6} per degree, resulting in a nonlinear shift in the frequency scale across the comb bandwidth. The bandwidth response of the detectors in the FTS will also affect the resolution of the instrument, introducing some systematic apodization prior to data retrieval [25].

Table 1. Contributions to optical uncertainties in the FTS

Source	Accuracy	Precision over 1-s acquisition time	Contribution in optical domain
RF synthesizer [26]	5×10^{-11}	3×10^{-11}	300 Hz
Diode laser [27]	-	2.6×10^{-9}	1.06 MHz
Rb-line [20]	1×10^{-10}	-	
CEO frequency [4]	-	5×10^{-9}	1 MHz
Air dispersion [21]	-	1×10^{-6}	1 kHz
Detector response [28]	-	-	Apodization

5. Conclusion

In summary, we have demonstrated a broadband, atomically traceable Fourier-transform spectrometer, capable of consistently identifying any subset of modes transmitted by a Fabry-Pérot etalon used to filter a frequency comb. This capability is needed by future high-resolution spectrographs such as ELT HIRES, whose ultra-broadband design implies the need for multiple Fabry-Pérot cavities operating at diverse wavelengths, rendering impractical the current referencing paradigm based on co-locking a narrow-line cw laser with the comb.

Cross-correlation analysis of the filtered comb with the 1.27-GHz instrument line shape enabled each comb-line position to be identified with a precision of 17.6 MHz, equivalent to 34 fm at 800 nm. The resolving power of ~2 pm in the optical domain is comparable with VIPA technology [29].

The precision to which individual comb modes can be identified could be used to recover the refractive index of air by observing the frequency-dependent shift in the spacing between filtered comb lines prior to correction, potentially providing an *in situ* compensation method without prior knowledge of local pressure, humidity and temperature.

Funding

UK Science and Technologies Facilities Council (STFC) (ST/N000625/1, ST/N006925/1).